Interacting boson approximation-2 analysis of the Pd and Ru chains. I. Mixed symmetry states of $F_{max}-1$ character in even palladium isotopes

A. Giannatiempo
Dipartimento di Fisica, Università di Firenze e Istituto di Fisica Nucleare, Florence, Italy

A. Nannini
Istituto di Fisica Nucleare, Florence, Italy

P. Sona
Dipartimento di Fisica, Università di Firenze e Istituto di Fisica Nucleare, Florence, Italy

(Received 3 February 1998; revised manuscript received 1 July 1998)

An analysis of positive parity levels in the even palladium isotopes $^{100-116}$Pd has been carried out in the framework of the interacting boson approximation-2 model to identify states having large mixed-symmetry components. By means of numerical calculations, performed in the U(5) limit of the model, it has been possible to find simple relations obeyed by the eigenvalues of the generalized Majorana operator for the mixed-symmetry states having $F=F_{max}-1$. These results have been utilized as a starting point for our analysis. Experimental energies, static and transition electric quadrupole and magnetic dipole moments as well as mixing ratios and intensity ratios have been compared to the values calculated by using a realistic Hamiltonian. In the analysis only six out of the twelve model parameters have been varied as a function of the neutron number. A good overall agreement has been found. A detailed investigation of the level structure made it possible to identify whole groups of states of predominant mixed-symmetry character and to establish, in most cases, a close correspondence with states of the U(5) limit of the model. [S0556-2813(98)02412-1]

PACS number(s): 21.60.Fw, 21.10.Re, 27.60.+j

I. INTRODUCTION

The interacting boson model, in its early version IBA-1 [1], which is fully symmetric in the proton and neutron degrees of freedom, has been very successful in reproducing the properties of many low-lying positive parity levels in medium and heavy even-even nuclei [2]. However, even a simple inspection of the excitation-energy patterns at rather low energy (say $\leqslant 3$ MeV) reveals the presence of levels which cannot be interpreted in the IBA-1 model space. The IBA-2 extension of the model predicts a new class of states [3,4] having mixed symmetry (MS) in the proton and neutron degrees of freedom, some of which could possibly be identified with the additional states.

An investigation aimed at clarifying to what extent the IBA-2 model can describe positive parity states in even-even medium and heavy nuclei needs a systematic comparison of experimental data and theoretical predictions, e.g., over an isotopic chain. In this case the parameters of the adopted model Hamiltonian and transition operators are requested to vary smoothly from one isotope to the next, thereby reducing the possibility of achieving ''fictitious'' good agreement with experimental data by fine tuning the parameters for each isotope. Moreover, by considering a whole isotopic chain (or, better, several neighbouring ones) the difficulties arising from the lack of important experimental data may be attenuated.

Some years ago we started, in the framework of the IBA-2 model, an investigation of nuclei having a proton number close to $Z=50$. From the analysis of energies, static moments, transitions rates and mixing ratios in ^{110,112,114}Cd isotopes ($Z=48$) we found evidence for identifying the 2_3^+ state as the lowest state of MS character [5]. Later on, our analysis of the $B(E0)/B(M1)$ ratios in the $2_3^+ \rightarrow 2_1^+$ transitions supported this interpretation [6]. We thus extended our study to even $^{98-114}$Ru isotopes ($Z=44$) providing a large body of evidence for assigning to several levels an MS character [7]. In particular, the 2_3^+ state has been shown to be the lowest state of MS character all along the isotopic chain; the 3_1^+ level has been found to be the lowest odd-spin state having a large MS component and, in the heavier isotopes of the chain, a band of MS states having $J^\pi=5^+$, 7^+, and 9^+ above this level has been identified. Sizable MS components have also been found for the 6_2^+ and 8_2^+ states.

In this work we present the results of our study of $^{100-116}$Pd isotopes ($Z=46$). A preliminary account of some aspects of this work has been presented in [8].

A systematic analysis of even palladium isotopes, in the framework of the IBA-2 model, has been performed a long time ago by Van Isacker and Puddu [9] who only considered fully symmetric (FS) states. Recently, results of IBA-2 calculations on $^{102-116}$Pd isotopes have been published by Kim *et al.* [10].

II. PROPERTIES OF $F=F_{max}-1$ STATES IN THE U(5) LIMIT

As pointed out by several authors (e.g., [10,11]), even palladium isotopes belong to a region of transition from the U(5) to the O(6) limit of the IBA model. These limits correspond, in a geometrical picture, to anharmonic vibrational and γ unstable nuclei, respectively.

The problem of the identification of MS states other than the lowest ones has been faced, for the first time, in our work on ruthenium isotopes [7] where, due to the lack of specific guidelines, we referred to the U(5) limit of the model to obtain information on the properties which possible candidates should possess.

In the U(5) limit, states are characterized [2] by the quantum numbers

$$[N_\nu]\times[N_\pi]\ \ [N-f,f]\ \ \{n_1,n_2\}\ \ (v_1,v_2)\ \ \alpha\ \ L,$$

which label the irreducible representations of the groups in the chain

$$U_\nu(6)$$
$$\times U_\pi(6)\supset U_{\nu+\pi}(6)\supset U_{\nu+\pi}(5)\supset O_{\nu+\pi}(5)\supset O_{\nu+\pi}(3). \tag{1}$$

Here N_ρ $(\rho=\pi,\nu)$ is the number of ρ bosons, $N=N_\pi+N_\nu$ and α is a label necessary to completely specify the $O_{\nu+\pi}(5)\supset O_{\nu+\pi}(3)$ reduction.

Instead of the the quantum numbers $[N-f,\ f]$ one can use the quantities $[N,\ F]$, the F-spin quantum number being related to f by the expression $F=N/2-f$ [12].

Fully symmetric states have the maximum value of the F-spin ($F_{\max}=N/2$) and are equivalent to the IBA-1 states with the same value of N. Mixed-symmetry states are characterized by quantum numbers $F=F_{\max}-1,\ F_{\max}-2\ldots,$ down to the minimum value given by $F_{\min}=1/2\ |N_\pi-N_\nu|$.

The simplest form of the Hamiltonian in the U(5) limit is given by

$$H=\varepsilon(\hat{n}_{d\pi}+\hat{n}_{d\nu})+\hat{M}_{\pi\nu}. \tag{2}$$

Here $\hat{n}_{d_\rho}=(d^\dagger_\rho\cdot\tilde{d}_\rho)$ is the d-boson number operator and $\hat{M}_{\pi\nu}$ represents the Majorana operator which has zero eigenvalues when applied to FS states and is responsible for the shift in excitation energy of MS states with respect to FS states. In the most general form it is given by

$$\begin{aligned}\hat{M}_{\pi\nu}=&\tfrac{1}{2}\xi_2[s^\dagger_\nu\times d^\dagger_\pi-s^\dagger_\pi\times d^\dagger_\nu]^{(2)}\cdot[\tilde{s}_\nu\times\tilde{d}_\pi-\tilde{s}_\pi\times\tilde{d}_\nu]^{(2)}\\&+\xi_1[d^\dagger_\nu\times d^\dagger_\pi]^{(1)}\cdot[\tilde{d}_\nu\times\tilde{d}_\pi]^{(1)}\\&+\xi_3[d^\dagger_\nu\times d^\dagger_\pi]^{(3)}\cdot[\tilde{d}_\nu\times\tilde{d}_\pi]^{(3)},\end{aligned} \tag{3}$$

where ξ_1,ξ_2,ξ_3 are the so-called Majorana parameters. For increasing values of these parameters mixed-symmetry states move to higher energy.

The eigenvalues of $\hat{M}_{\pi\nu}$ have been given in closed form only for the particular case $\xi_1=\xi_3=-\xi_2$ [13].

Having realized in our previous analyses the importance of using unconstrained Majorana parameters for the identification of MS states, we diagonalized the Hamiltonian (2) to find out whether analytic expressions were obeyed by the eigenvalues of the generalized Majorana operator (3). Calculations were performed by using the NPBOS code [14]. As a result, we found that all states having $F=F_{\max}-1$ can be arranged in three groups, according to the different dependence of their excitation energies on ξ_1,ξ_2,ξ_3. For two of these groups the eigenvalues of the Hamiltonian (2) can be given in a closed analytic form depending only on ξ_2 and ξ_3. For the third group the excitation energy depends on all the Majorana parameters according to an expression of the type

$$E=\varepsilon n_d+\frac{1}{2}N\xi_2+\frac{1}{2}n_d(-\xi_2+\xi_1)+\zeta(-\xi_1+\xi_3), \tag{4}$$

where ζ is a positive coefficient which depends on the number of d-bosons and assumes different values for states having the same n_d. For any given n_d, its value is smaller than $1/2\ \ n_d$, so that the total coefficient of ξ_1 in Eq. (4) is positive.

In Fig. 1 are reported the excitation-energy pattern of FS states and of the three groups of MS states having $F=F_{\max}-1$ for a nucleus having $N=7$. States are displayed in separate columns according to the expressions obeyed by their energy eigenvalues, which are reported in the lower part of the figure. In each column, the full range of n_d values allowed by the labels of the irreducible representations of the U(6) and U(5) groups (given in the upper part of the figure) is reported. For a given n_d, in columns (a) and (a′), (b′) are displayed the five FS states and the three MS states of highest spin. We remark that the $n_d=3$ multiplet in column (b′) is composed of only three states. States of column (c′) can be grouped in different subsets distinguished by the expression of the coefficient ζ in Eq. (4): in Fig. 1 we display only the energy of the two subsets of states which, for any given n_d, have the highest and second highest spin value.

States in columns (a), (a′), (b′) belong to degenerate multiplets characterized by the number of d-bosons. States in columns (a′) are the counterpart of the states in column (a) having the same spin and d-boson number. The spacing $S_{a'}$ between MS multiplets in column (a′) is the same as that of FS multiplets in column (a) ($S_{a'}=S_a=\varepsilon$). The spacing $S_{b'}$ between multiplets in column (b′) depends on ξ_2, ξ_3 and is given by $S_{b'}=\varepsilon+1/2(-\xi_2+\xi_3)$.

As long as ξ_2 is positive and ξ_3 negative (which is the case in the following analysis) the spacing $S_{b'}$ is smaller than S_a so that states of columns (b′) can become yrast. For example, in the case reported in the figure, the odd-spin yrast band, starting from the 5^+ state, is made-up by the states of highest spin in each multiplet of column (b′). This is not the case for states of column (a′) whose n_d-multiplets are always higher in energy than the corresponding ones in column (a).

The regularities we found in spectra of the Majorana operator for states of columns (a′), (b′) and for the lowest states of column (c′) have been explained by Talmi [15] on the basis of partial dynamic symmetries of the IBA-2 Hamiltonian in the $U_{\nu+\pi}(5)$ limit.

A safe identification of a class of states relies not only on the comparison of predicted and observed excitation-energy patterns but also on a detailed analysis of their decay modes.

In the IBA-2 model $E2$ and $M1$ operators are expressed as [2]

$$\begin{aligned}\hat{T}(E2)\ \equiv&e_\nu\ \hat{T}_\nu(E2)+e_\pi\ \hat{T}_\pi(E2)\\=&e_\nu\hat{Q}_\nu+e_\pi\hat{Q}_\pi,\end{aligned} \tag{5}$$

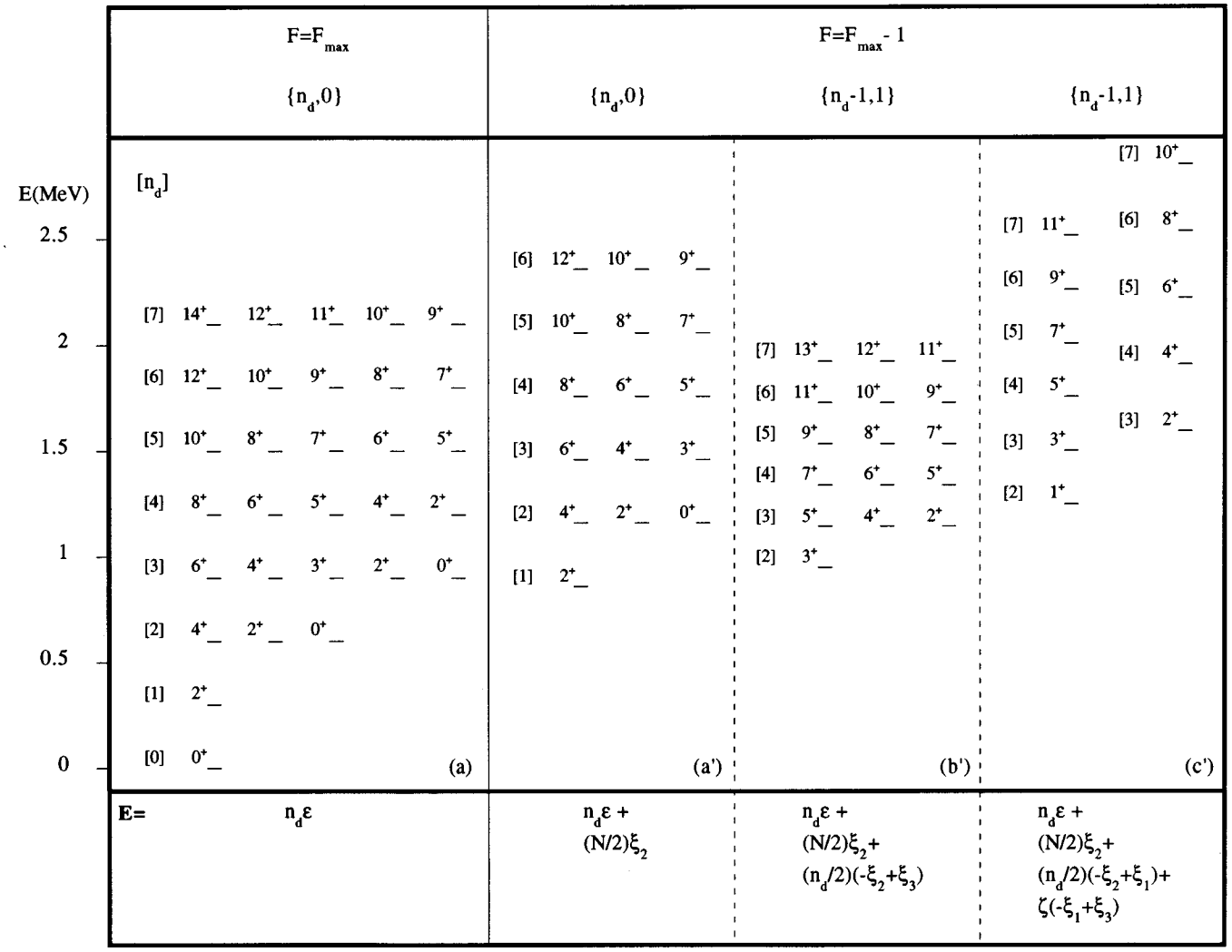

FIG. 1. Excitation energies of FS states and MS states having $F=F_{\max}-1$ in the U(5) limit, for the particular case $N_\pi=2$, $N_\nu=5$. Expressions reported at the bottom of the figure are valid in the U(5) limit for any N. The parameters used in the Hamiltonian are $\varepsilon=0.300$ MeV, $\xi_1=0.250$ MeV, $\xi_2=0.160$ MeV, $\xi_3=-0.055$ MeV. MS states are reported in columns according to their different dependence on the Majorana parameters, given in the lower part. At the top of each column are shown the quantum numbers $\{n_1,n_2\}$ of the relevant $U_{\nu+\pi}(5)$ representation. The number of d-bosons is reported in square brackets. In column (c′) $\zeta=0.30(nd-2)$ for odd spin states and $\zeta=0.10(nd-3)$ for even spin states.

$$\hat{T}(M1) \equiv g_\nu \hat{T}_\nu(M1)+g_\pi \hat{T}_\pi(M1) = \sqrt{\frac{3}{4\pi}}(g_\nu \hat{L}_\nu+g_\pi \hat{L}_\pi), \tag{6}$$

where

$$\hat{Q}_\rho=[d_\rho^\dagger\times\tilde{s}_\rho+s_\rho^\dagger\times\tilde{d}_\rho]^{(2)}+\chi_\rho[d_\rho^\dagger\times\tilde{d}_\rho]^{(2)}, \tag{7}$$

$$\hat{L}_\rho=\sqrt{10}[d_\rho^\dagger\times\tilde{d}_\rho]^{(1)}. \tag{8}$$

In these expressions χ_ρ is an adimensional coefficient, e_ρ and g_ρ are the effective quadrupole charges and gyromagnetic ratios and $\hat{L}$ is the angular momentum operator.

Because of the form of the transition operators, $E2$ transitions obey the selection rule $\Delta n_d=0,\pm1$ while $M1$ transitions can only connect states having the same d-boson number.

Both $E2$ and $M1$ transitions obey the F-spin selection rule $\Delta F=0,\ \pm1$; moreover $M1$ transitions are forbidden between FS states [16,17]. The reduced matrix elements $\langle\|\hat{T}_\nu\|\rangle$ and $\langle\|\hat{T}_\pi\|\rangle$ of the $M1$ transition operator have always the same absolute values but opposite signs [17], so that $M1$ transition probabilities are proportional to $(g_\pi-g_\nu)^2$. As to $E2$ transitions, the relation $\langle\|\hat{T}_\nu\|\rangle=-\langle\|\hat{T}_\pi\|\rangle$ holds when $\Delta F=\pm1$ [18]; in this case $E2$ transition probabilities between states having the same d-boson number will be proportional to $(e_\nu\chi_\nu-e_\pi\chi_\pi)^2$, while those between states differing by one d-boson will be proportional to $(e_\nu-e_\pi)^2$.

In the U(5) limit, expressions for the electromagnetic properties of low lying states of columns (a′), (b′), (c′) have been derived in closed form in [18–20]. It turns out that $E2$ transitions between $F=F_{\max}-1$ states are of the same order of magnitude as those between FS states.

The properties just discussed provide useful signatures for the identification of states having $F=F_{\max}-1$ character in nuclei having a structure close to the U(5) limit. For ex-

ample, the identification of the lowest lying 2^+ MS state in nuclei having a vibrational structure has been based on the presence of a strong $M1$ component (therefore on a small value of the $E2/M1$ mixing ratio δ) in the transition to the 2_1^+ state (see, e.g., [17] and references therein).

III. PARAMETERS OF THE IBA-2 MODEL

For the present calculations we adopted the same Hamiltonian as in our previuos work on the ruthenium chain [7], namely

$$H=\varepsilon\,(\hat{n}_{d_\pi}+\hat{n}_{d_\nu})+\kappa\,\hat{Q}_\pi\cdot\hat{Q}_\nu+w_{\pi\nu}\hat{L}_\pi\cdot\hat{L}_\nu+\hat{M}_{\pi\nu}. \quad (9)$$

With respect to the Hamiltonian (2) there are two additional terms representing the quadrupole and dipole interactions between neutron-boson and proton-boson. Because of these terms, the Hamiltonian is no longer an F-scalar so that the wavefunction of a state can have different F-spin components.

Calculations have been performed by using the NPBOS code [14] which gives the structure of the wave function of each state in terms of the number of d-boson and F-spin components. Even palladium isotopes have two proton-bosons and a number of neutron-bosons which reaches a maximum of eight for the neutron number $N=66$, half way between the closed shells at $N=50$ and $N=82$. For $A \geqslant 100$ the possible F-spin values range from $F_{\max}$ to $F_{\max}-2$.

The parameters ε, κ, $w_{\pi\nu}$, ξ_2, ξ_3 have been determined so as to reproduce as closely as possible the excitation-energy of all positive parity levels for which a clear indication of the spin value exists, following the same procedure described in [7]. For the final choice of the parameters χ_π and χ_ν, their influence on quadrupole moments and $E2/M1$ mixing ratios has also been taken into account. The value of χ_π has been kept fixed along the isotopic chain as suggested by microscopic considerations which predict that this parameter depends only on the proton number [21]. The final adopted value ($\chi_\pi=-0.9$) is close to that found ($\chi_\pi=-0.8$) for the ruthenium chain.

TABLE I. Adopted values for the Hamiltonian parameters used for IBM-2 calculations. All parameters are given in MeV, except χ_ν (dimensionless). The values of the parameters kept fixed along the isotopic chain are $\chi_\pi=-0.90$ and $\xi_1=1.0$ MeV.

A	ε	κ	χ_ν	$w_{\pi,\nu}$	ξ_2	ξ_3
100	0.785	−0.06	−1.10	0.000	0.33	−0.32
102	0.760	−0.08	−1.10	0.015	0.28	−0.29
104	0.800	−0.08	−0.65	0.030	0.24	−0.28
106	0.741	−0.08	−0.55	0.030	0.20	−0.25
108	0.678	−0.08	−0.50	0.040	0.12	−0.25
110	0.624	−0.08	−0.40	0.050	0.11	−0.20
112	0.604	−0.10	0.10	0.060	0.00	−0.19
114	0.547	−0.10	0.20	0.060	0.01	−0.18
116	0.550	−0.10	0.20	0.060	0.05	−0.16

The parameter ξ_1 was fixed at a value sufficiently high to push the lowest 1^+ MS state at an energy $\geqslant 2$ MeV, due to the fact that no $J^\pi=1^+$ level has been definitely identified below this energy in all isotopes here examined. We have also checked that the calculated excitation-energies of the levels relevant to this work do not depend on the value of ξ_1 when it is varied over a large range of positive values centered around 1 MeV.

The effective quadrupole charges have been deduced through a minimum χ^2 procedure performed in the way described in [7]. Their values ($e_\pi=0.095$, $e_\nu=0.115$ e b) are close to those found for the ruthenium chain ($e_\pi=0.080$, $e_\nu=0.120$ e b). For the effective gyromagnetic ratios we adopted the values derived in [7], namely $g_\pi=0.51$ and $g_\nu=0.28$ μ_N.

The full set of adopted parameters is reported in Table I. Altogether, six out of twelve parameters appearing in the

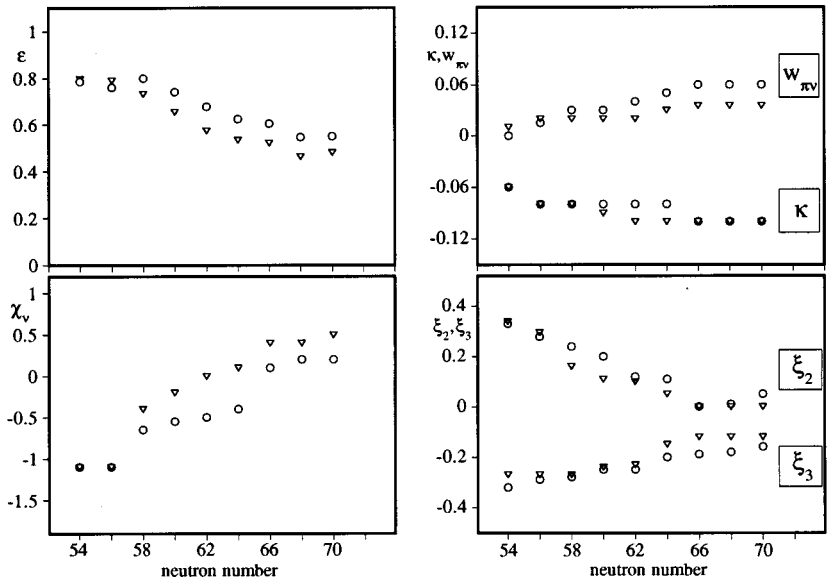

FIG. 2. The adopted values of the Hamiltonian parameters which have been varied along the isotopic chain are shown as a function of the neutron number for palladium (circles) and ruthenium (triangles) isotopes. The parameters $\varepsilon,\kappa,w_{\pi\nu},\xi_2,\xi_3$ are reported in MeV. Data on ruthenium isotopes are taken from [7].

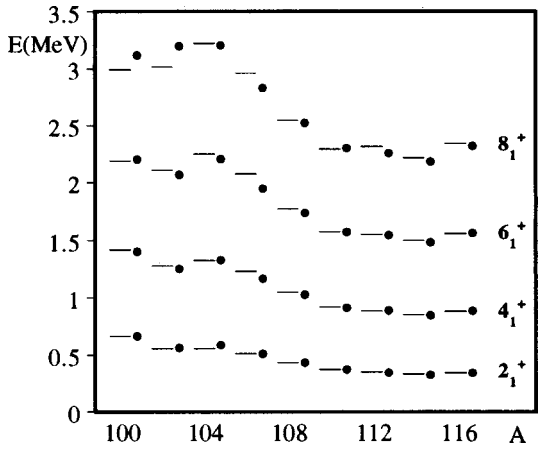

FIG. 3. Experimental excitation energies of the even-spin yrast states up to $J=8$ in the palladium chain are compared to the calculated values.

Hamiltonian and in the $E2$ and $M1$ operators have been kept fixed along the isotopic chain. In Fig. 2 the values of the remaining parameters are reported as a function of the neutron number together with the corresponding values for ruthenium isotopes. One can observe the following.

They have quite similar values for isotones of the two isotopic chains and vary smoothly from an isotope to the neighboring one.

κ varies over a quite restricted range with a maximum absolute value of 0.1 MeV.

The behavior of χ_ν is that expected on the basis of microscopic calculations [21], i.e., it has negative values of large magnitude at the beginning of the neutron shell and rises to positive values beyond half shell.

ξ_2 and ξ_3 show the same trend found for the ruthenium chain: ξ_2 has large, positive values at the beginning of the neutron shell and decreases monotonically towards the middle of the shell while ξ_3 displays the opposite trend.

The values of both ξ_2 and ξ_3 fall in a narrow band thereby defining a region of reasonable values for these parameters in the $A=100-120$ mass region.

An important starting point for establishing the presence of states of MS character is to investigate whether there are states whose excitation energies can be reproduced by a suitable choice of the Majorana parameters. To disentangle the effect of the latter from that due to the remaining Hamiltonian parameters, we first checked whether the predicted excitation energy of states whose wave functions have a predominant $F=F_{\max}$ component (thus being very little affected by ξ_2 and ξ_3) is close to the experimental ones. A general idea of the agreement of experimental and calculated excitation energies for the even-spin yrast states up to $J=8$ (they turn out to be of FS character) can be obtained from Fig. 3. We then considered the influence of ξ_2 and ξ_3 on the excitation energy of the remaining states for all the palladium isotopes studied in this work and in each case very important information has been gained for identifying possible MS candidates.

To illustrate the procedure that has been followed, the most useful example is that of ^{106}Pd, since an ample experimental information is available on its excitation-energy pattern, which is shown in Fig. 4. For the sake of clarity, groups

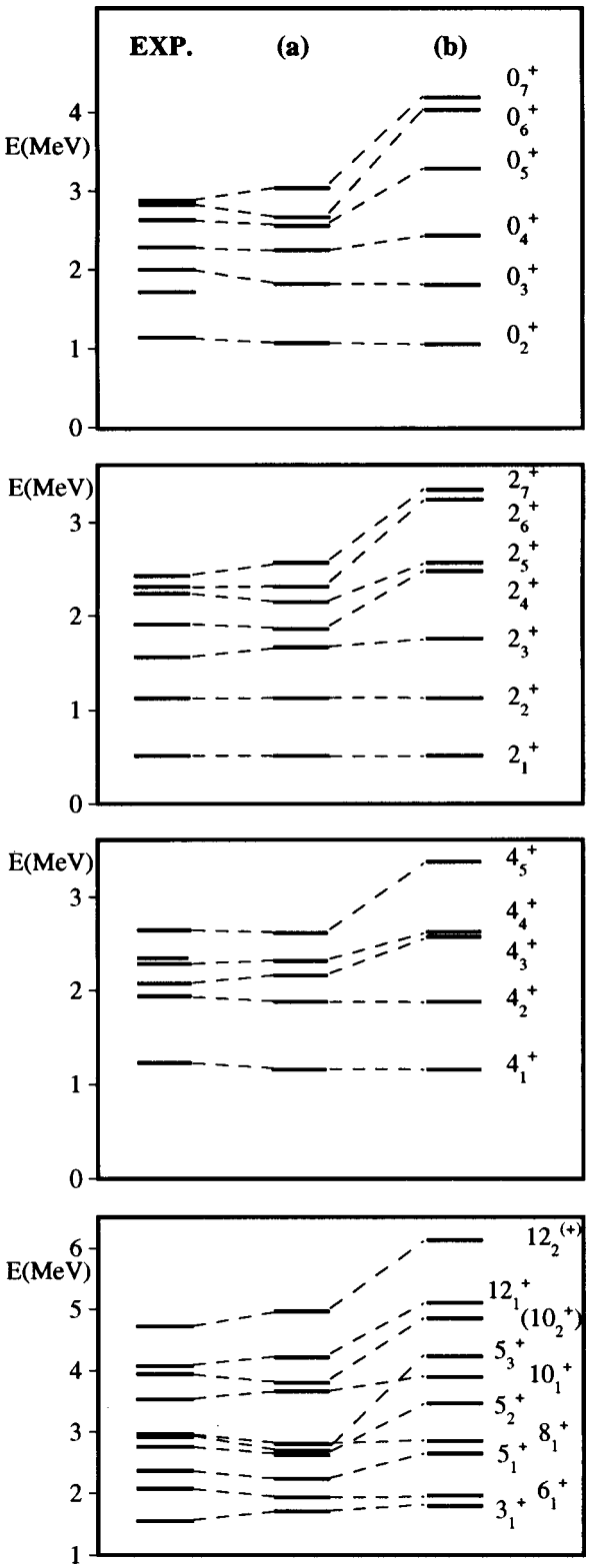

FIG. 4. Experimental values of the excitation energies of positive parity levels in ^{106}Pd are compared to those calculated by using the Hamiltonian parameters given in Table I [column (a)] and those obtained by setting $\xi_2=\xi_3=1$ MeV [column (b)]. The two states which have no connecting line are interpreted as lying outside the standard IBA-2 model space.

of states of a given spin are reported in separate boxes. The experimental data include all positive parity levels up to 2.5 MeV (they all have definite spin assignement) and, above

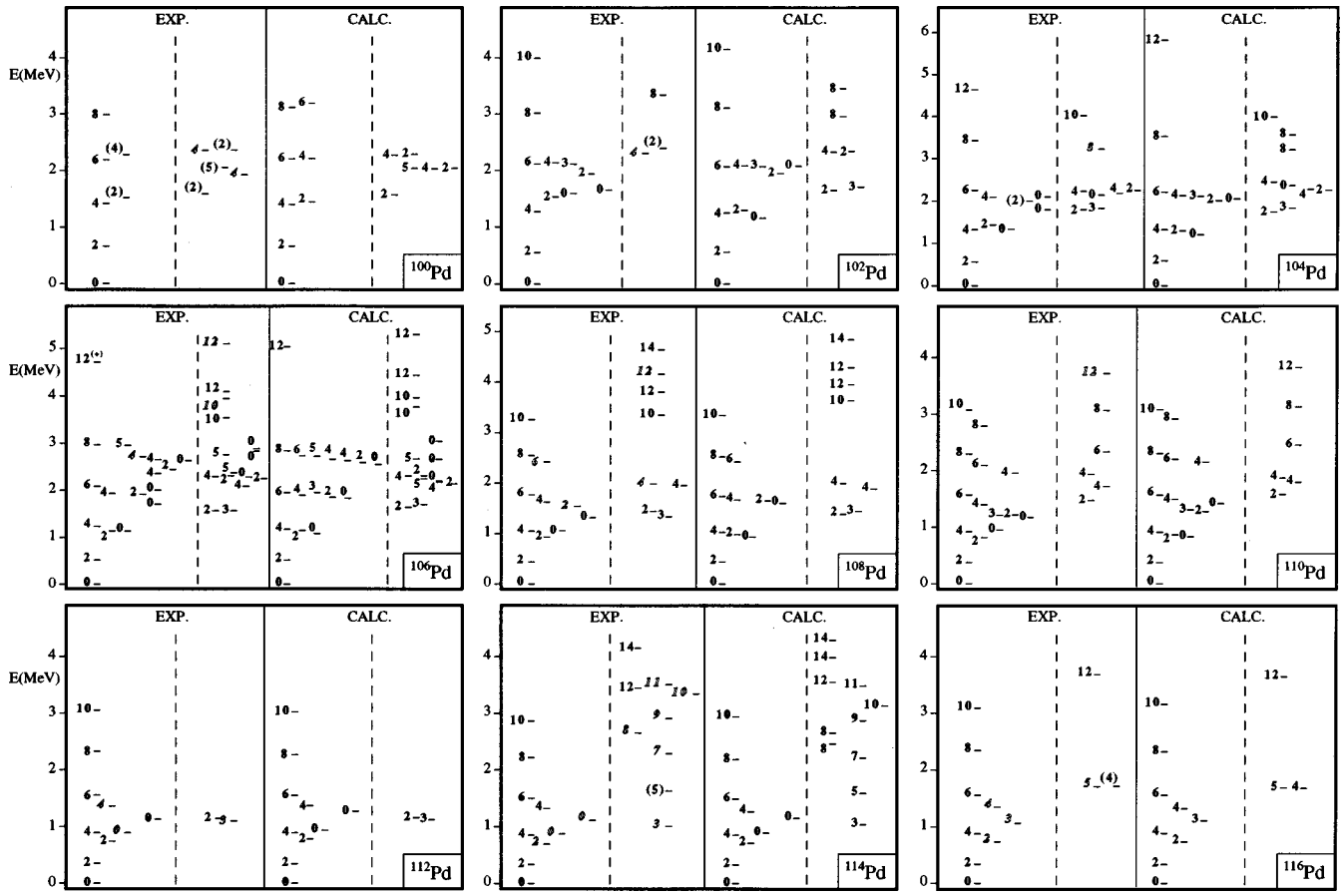

FIG. 5. Experimental and calculated excitation energies for positive parity states in $^{100-116}$Pd. Full (open) character on the left part of the figure refer to experimental states whose spin and parity have been uniquely assigned (proposed); when several spin assignments are consistent with experimental data the assumed value is reported in brackets.

this energy, only those of definite spin J_i with no ambiguity on the ordinal i induced by uncertainties about the spin of lower lying states. In the figure their excitation energy is compared to that calculated by using the adopted set of parameters [column (a)] or the set obtained by changing only the Majorana parameters to the values $\xi_2=\xi_3=1$ MeV [column (b)]. With the latter choice, all states in column (b) have an $F_{\max}$ component (amplitude square) larger than 0.98, since all MS states have been moved to much higher energy. It is seen how the agreement with the experimental data dramatically improves in passing from column (b) to (a).

IV. EXCITATIONS ENERGIES AND ELECTROMAGNETIC PROPERTIES

The comparison of experimental and calculated energies of positive parity states in $^{100-116}$Pd is given in Fig. 5. Experimental data are taken from the following references: ^{100}Pd [23], ^{102}Pd [24], ^{104}Pd [25,26], ^{106}Pd [27,28], ^{108}Pd [28–30], ^{110}Pd [28,31–33], ^{112}Pd [34,35], ^{114}Pd [35,36], ^{116}Pd [35,37].

For each isotope all the experimental energies of positive parity states up to that of the $J_i^+=6_1^+$ level are reported in the figure. Above this energy, up to 5 MeV, we only display, as a rule, states having $J\geqslant 4$ with definite or strongly suggested spin assignement and definite value of the ordinal i. Experimental energies are reported on the left part of the figure and the calculated ones on the right part. The latter are grouped in two columns: states of predominant FS character are reported on the left of the dashed line, while those of predominant MS character are given on the right. The experimental levels are also arranged in two columns so as to display clearly our proposed correspondence.

As to the e.m. properties, the experimental values of electric quadrupole and magnetic dipole moments of the relevant states of each isotope as well as $B(E2)$ and $B(M1)$ reduced transition probabilities, $E2/M1$ mixing ratios and intensity ratios for the deexciting transitions have been compared to the calculated ones. In this analysis we used for χ_π and χ_ν in the expression of the E2 operator (5) the same values (consistent-Q formalism [2]) as in the Hamiltonian (9).

The relevant experimental data for each isotope are from the same references given above, except for the two possible values of $\delta(3_1^+\rightarrow 2_1^+)$ in ^{104}Pd [38].

All available experimental data on magnetic dipole moments and $B(M1)$'s are reported in Table II together with the corresponding calculated values.

The experimental and predicted values of the electric quadrupole moments Q and $B(E2)$ reduced transition probabilities are shown in Figs. 6,7. The $B(E2)$ values are displayed on a logarithmic scale since their values vary over 4 orders of magnitude.

The $E2/M1$ mixing ratios, defined by the usual expression [22]

TABLE II. Experimental values of magnetic dipole moments μ (μ_N) and reduced transition probabilities $B(M1)$ (μ_N^2) are compared to the calculated ones for even palladium isotopes. The values $g_\pi = 0.51$ μ_N, $g_\nu = 0.28$ μ_N for the effective giromagnetic ratios have been used. The calculated value of $B(M1;\ 2_2^+ \to 2_1^+)$ in ^{102}Pd is reported in italics since the interpretation of the 2_2^+ level in the framework of the model is doubtful (see text). The experimental B(M1) values of the $2_2^+ \to 2_1^+$ transition in ^{104}Pd and $2_3^+ \to 2_1^+$, $4_2^+ \to 4_1^+$ transitions in ^{106}Pd have been deduced from the relevant values of $B(E2)$ and δ^2 [24,25,26]. The limit for $B(M1;\ 2_3^+ \to 2_1^+)$ in ^{104}Pd has been deduced from the relevant values of $B(E2;\ 2_3^+ \to 0_1^+)$ and of the branching ratio [24] in the hypotehsis that the $2_3^+ \to 2_1^+$ transition has a pure $M1$ multipolarity.

A	$\mu(2_1^+)$		$B(M1;\ 2_2^+ \to 2_1^+)$		$B(M1;\ 2_3^+ \to 2_1^+)$		$B(M1;\ 4_2^+ \to 4_1^+)$	
	Expt.	Calc.	Expt.	Calc.	Expt.	Calc.	Expt.	Calc.
102	0.82(8)	0.76	0.0036(7)	*0.00001*				
104	0.82(6)	0.74	0.0011(19)	0.0002	$>$0.013	0.015		
106	0.80(4)	0.72	0.0004(2)	0.0002	0.021(4)	0.011	0.0045(6)	0.0003
108	0.72(6)	0.70	0.0043(11)	0.0004				
110	0.62(6)	0.70	0.0011^{+11}_{-5}	0.0003				

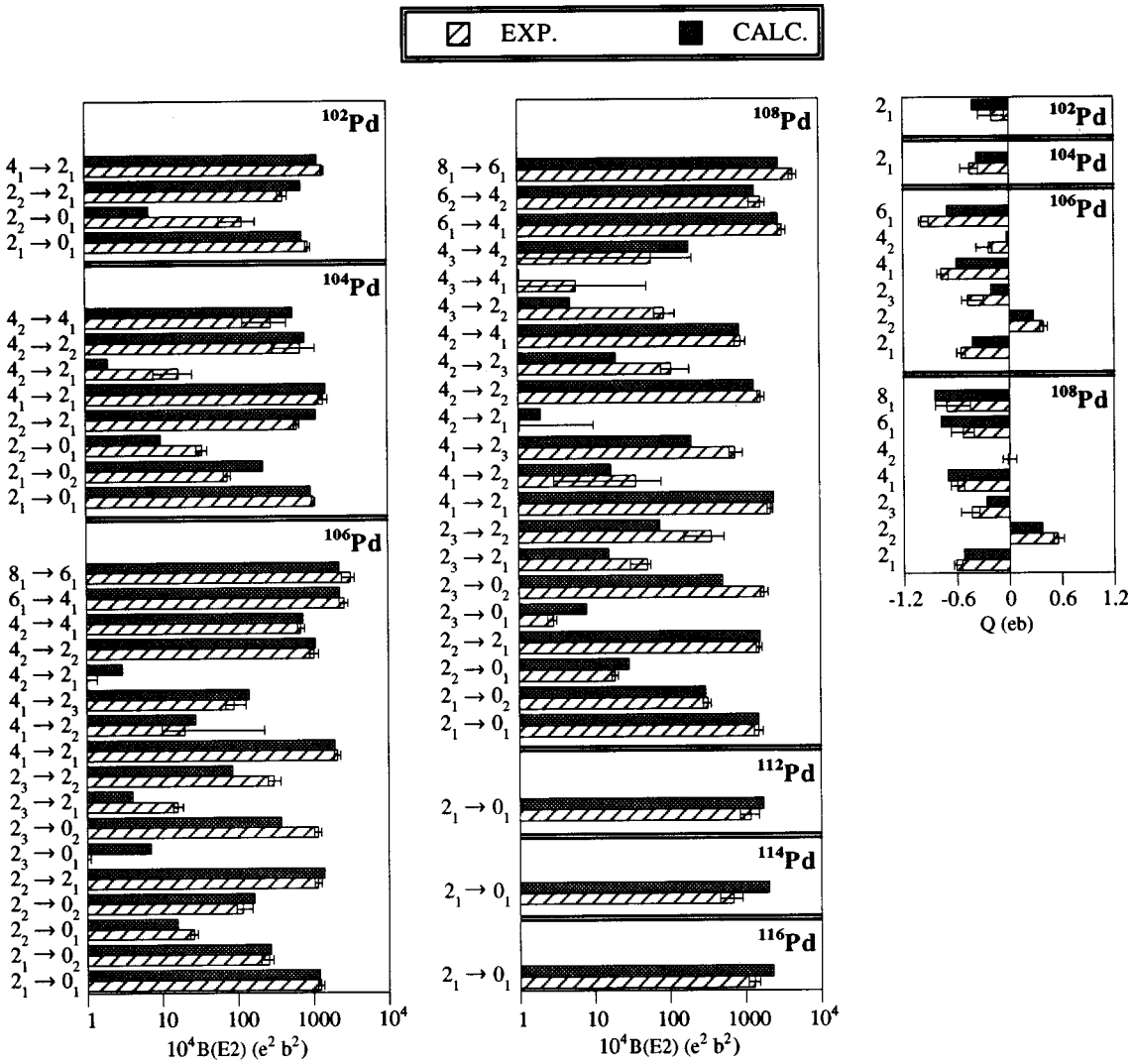

FIG. 6. Experimental and calculated values for $B(E2)$ reduced transition probabilities of the indicated transitions and electric quadrupole moment of the indicated levels in ^{102,104,106,108,112,114,116}Pd.

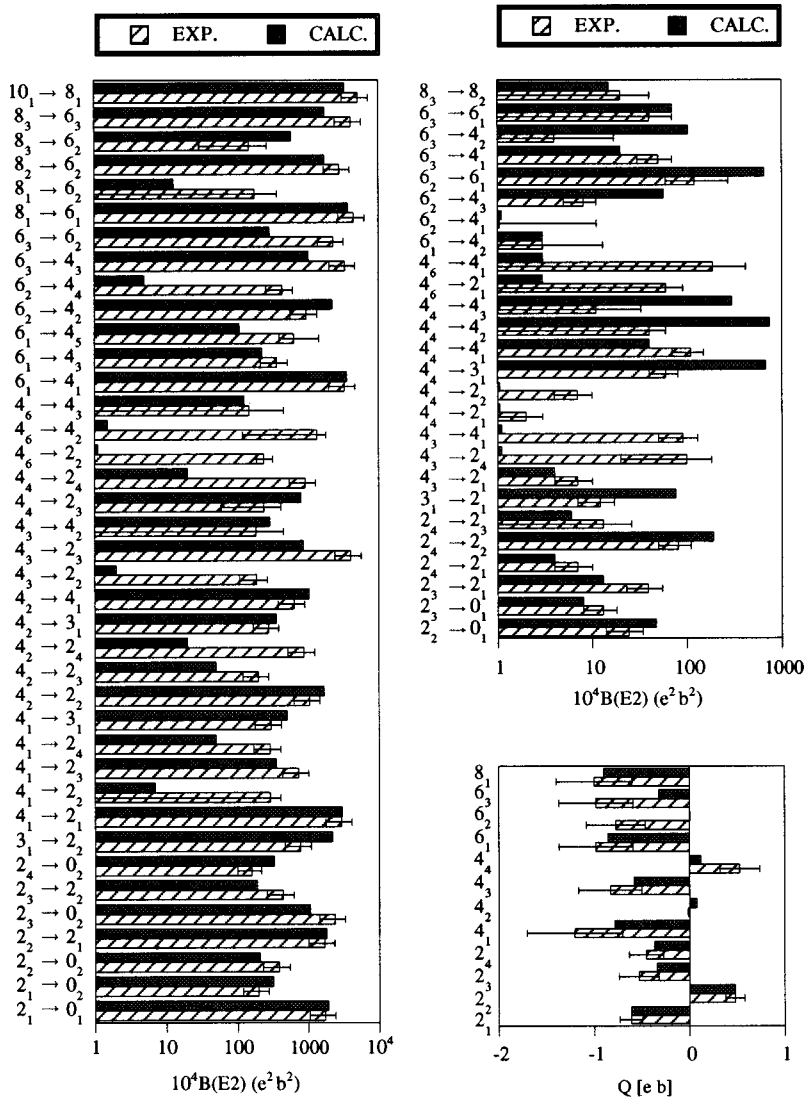

FIG. 7. As in Fig. 6 for ^{110}Pd. To help in the comparison, data concerning experimental $B(E2)$ values larger than 10^{-2} e^2 b^2 are reported on the left, the remaining ones on the right side of the figure. Experimental values are deduced from the data reported in [32].

$$\delta(J_i^\pi \to J_f^\pi) = -0.835 E_\gamma(\mathrm{MeV}) \frac{\langle J_f^\pi \| \hat{T}(E2) \| J_i^\pi \rangle \ \ (e\ \mathrm{b})}{\langle J_f^\pi \| \hat{T}(M1) \| J_i^\pi \rangle \ \ (\mu_N)} \tag{10}$$

are given in Table III together with intensity ratios. In this table, to make it apparent the contributions of the $E2$ and $M1$ strenghts to the observed branching ratio we report, for each transition, besides the calculated values of $B(M1)$ and $B(E2)$, the absolute transition probabilities

$$W_\gamma(M1) = 1.76 \times 10^{13} \ E_\gamma^3(\mathrm{MeV}) \ B(M1) \quad \mathrm{s}^{-1}, \tag{11}$$

$$W_\gamma(E2) = 1.22 \times 10^{13} E_\gamma^5(\mathrm{MeV}) \ B(E2) \quad \mathrm{s}^{-1}. \tag{12}$$

We note the general good agreement between the calculated and experimental data. We must mention that spectroscopic data concerning the 0_2^+ state in ^{102} Pd and the 4_5^+ state at 2.350 MeV in ^{110}Pd have not been included in Figs. 6,7 and Table III since the model fails to reproduce their properties. Indeed, the 0_2^+ state has a strongly hindered decay to the 2_1^+ state [$B(E2;\ 0_2^+ \to 2_1^+) < 4 \times 10^{-4}$ W.u.] and a strong $E0$ transition to the ground state, so that it clearly lies outside the IBA-2 model space, as already remarked in [39,10]. In ^{110}Pd the calculations predict only four 4^+ states in the energy region between 2.2 and 3 MeV whereas five are experimentally known. By comparing experimental and calculated decay properties we are led to conclude that the 4_5^+ state lies outside the IBA-2 model space.

V. DISCUSSION OF THE RESULTS

We now discuss the results reported in the previous section with the aim of identifying the predominant symmetry character of as many states as possible. In particular, we will try to establish a correspondence between the states shown in Fig. 5 and the states of the U(5) limit given in Fig. 1. For the sake of simplicity, we will refer to this limit also for the heavier isotopes of the chain even though their structure appears to be slowly changing towards the O(6) limit of the model.

A. FS states

In this subsection we consider the states of spin $\leqslant 8$ reported on the left of the dashed lines in Fig. 5.

TABLE III. Experimental and calculated mixing ratios δ and relative intensities for γ transitions deexciting the indicated levels in $^{102-116}$Pd. The units for transition energies E_γ and reduced transition probabilities $B(M1)$, $B(E2)$ are MeV, $10^{-4}\mu_N^2$ and 10^{-4} e^2 b^2, respectively. The calculated $M1$ and $E2$ transition probabilites (in 10^9 s^{-1}) are given in columns 9 and 10. The values $e_\pi = 0.095$, $e_\nu = 0.115$ e b for the effective charges and $g_\pi = 0.51$, $g_\nu = 0.28$ μ_N for the effective giromagnetic ratios have been used. Calculated data concerning the 2_2^+ level in ^{102}Pd are reported in italics since the interpretation of this state in the framework of the model is doubtful (see text).

A	J_i^π	J_f^π	E_γ	δ		$B(M1)$	$B(E2)$	$W_\gamma(M1)$	$W_\gamma(E2)$	Relative intensities	
				Calc.	Expt.					Calc.	Expt.
102	2_2^+	0_1^+	1.535				*7*		*73*	*100*	100(10)
		2_1^+	0.978	*−72*	2.8(2)	*0.7*	*733*	*0.3*	*830*	*1077*	97(8)
	3_1^+	2_1^+		8	$\geqslant 15$						
104	0_5^+	2_1^+	1.538				9		113	100	100(6)
		2_2^+	0.797				0.7		0.3	0.2	
		2_3^+	0.343				401		2.3	2	
	2_2^+	0_1^+	1.342				10		52	13	86(5)
		2_1^+	0.786	−16	−4.8(42)	2	1120	2	412	100	100(6)
	2_3^+	0_1^+	1.794				6		130	25	10(1)
		0_2^+	0.460				87		2	0.4	4(1)
		2_1^+	1.238	0.2	M1	154	5	514	16	100	100(6)
	2_5^+	2_1^+	1.689			7	0.5	57	9	100	100(10)
		2_2^+	0.902			5	3	7	2	14	10(2)
	3_1^+	2_1^+	1.265	−1.6	0.23(7) or $\lvert\delta\rvert > 13$	6	13	20	53	100	100(10)
		2_2^+	0.479	−0.7	$M1,E2$	97	268	19	8	37	24(4)
		4_1^+	0.498	−0.4	$M1,E2$	72	80	16	3	25	77(8)
	4_2^+	2_1^+	1.527				2		23	13	85(8)
		2_2^+	0.740				815		221	125	95(5)
		4_1^+	0.759	−8	−0.84(24)	3	566	2	174	100	100(5)
	4_3^+	2_1^+	1.626				0.4		5	6	50(5)
		2_2^+	0.840				2		1	1	12(3)
		4_1^+	0.858	−0.02	0.45(30)	84	0.1	94	0.05	100	100(1)
	4_4^+	2_1^+	1.708				0.3		6	3	4(1)
		2_2^+	0.923				0.1		0.7	0.03	28(3)
		3_1^+	0.444			28	204	4	4	4	7(1)
		4_1^+	0.942	0.22	−0.64(14)	144	11	10	222	100	100()
		4_2^+	0.183			21	18	0.2	0.005	0.1	2(1)
106	0_2^+	2_1^+	0.622				1360		154	100	100
		2_2^+	0.006				839		7×10^{-9}	0	
	0_4^+	2_1^+	1.490				3		26	2.8	0.8(1)
		2_2^+	0.873				1480		915	100	100(1)
		2_3^+	0.439				33		0.7	0.1	2.9(5)
	0_5^+	2_1^+	1.766				12		255	100	100(2)
		2_2^+	1.150				0.8		2	1	9(1)
		2_3^+	0.716				704		162	63	29(1)
	2_2^+	0_1^+	1.128				16		36	24	54(1)
		2_1^+	0.616	−13	−9.4(20)	2	1410	0.9	152	100	100(2)
	2_3^+	0_1^+	1.562				7		74	33	10.4(1)
		0_2^+	0.429				374		7	2.9	4.5(1)
		2_1^+	1.050	0.17	0.24(1)	107	4	219	6	100	100(2)
		2_2^+	0.434			1	85	0.1	2	0.8	1.3(1)
		4_1^+	0.333				143		0.7	0.3	
	2_4^+	0_1^+	1.909				0.4		12	5	35(4)
		2_1^+	1.397			52	2	250	14	100	100(1)
		2_2^+	0.782			0.01	231	0.007	82	32	3(1)
	2_5^+	0_1^+	2.243				0.5		32	5	16(1)
		0_2^+	1.109				1		2.5	0.4	47(4)
		2_1^+	1.730			1	3	9	54	10	18(1)
		2_2^+	1.115	−2.0	$1.5^{+0.3}_{-0.2}$	51	232	123	487	100	100(7)

TABLE III. (*Continued*).

A	J_i^π	J_f^π	E_γ	δ		$B(M1)$	$B(E2)$	$W_\gamma(M1)$	$W_\gamma(E2)$	Relative intensities	
				Calc.	Expt.					Calc.	Expt.
		2_3^+	0.680	-6	$M1,E2$	13	393	7	70	13	78(14)
		3_1^+	0.684			50	142	28	26	9	43(2)
	2_6^+	0_1^+	2.309				1		95	95	$\leqslant 9$
		2_1^+	1.797	0.63	0.25(2)	7	1	71	28	100	100(2)
		2_2^+	1.180	0.44	$-0.06(12)$	91	2	25	5	30	53(1)
		3_1^+	0.751			1	453	0.8	132	134	4(1)
	3_1^+	2_1^+	1.046	-2.2	$-3.8(4)$	4	27	9	42	100	100(5)
		2_2^+	0.430	-1.4	$-7.9(8)$	59	906	8	16	48	45(1)
		4_1^+	0.328	-0.69	$E2+(M1)$	45	285	3	1	8	3.9(2)
	4_2^+	2_1^+	1.419				3		19	4	0.3(1)
		2_2^+	0.804				1080		444	100	100(4)
		2_3^+	0.374				26		0.2	0.1	2.1(3)
		4_1^+	0.703	-9.9	$-2.30(2)$	3	750	2	157	36	36(1)
	4_3^+	2_1^+	1.566				0.7		8	8	6(1)
		2_2^+	0.950				2		2	2	12(2)
		4_1^+	0.847			82	0.5	88	0.3	100	100(33)
	4_4^+	2_1^+	1.771				0.2		5	2	4(1)
		4_1^+	1.054	0.3	$M1,E2$	110	12	227	19	100	100(15)
	5_1^+	3_1^+	0.808				984		413	100	100(5)
		4_1^+	1.137			14	3	35	7	10	6(1)
		4_2^+	0.434			93	125	13	2	4	2(1)
	5_2^+	3_1^+	1.199				140		423	40	40(2)
		4_1^+	1.528	4.8	$-2.5(1)$	0	5	2	50	5	58(15)
		4_2^+	0.825	3.7	$-6.5(6)$	5	154	5	72	7	55(1)
		4_4^+	0.474	-1.3	$-4.0^{+0.9}_{-0.6}$	16	178	3	5	0.8	3.3(2)
		5_1^+	0.391	-0.8	$E2(+M1)$	32	176	3	2	0.5	13.3(5)
		6_1^+	0.680	-10	$M1,E2$	0	113	0.2	20	1.9	5.5(3)
	5_3^+	3_1^+	1.394				79		508	93	93(11)
		4_1^+	1.723	2.1	$-2.5(14)$	1	3	13	57	13	74(14)
		4_2^+	1.020	21	$M1,E2$	0	246	1	331	61	66(5)
		4_3^+	0.874			42	219	50	137	34	21(3)
		5_1^+	0.586	-1.9	$M1,E2$	8	125	3	10	3	28(3)
		5_2^+	0.195	0.22	$M1(+E2)$	30	55	0.4	0.02	0.1	19(2)
108	2_2^+	0_1^+	0.931				30		25	42	22(2)
		2_1^+	0.497	-8.3	$-3.1(4)$	4	1610	0.9	60	100	100(2)
	2_3^+	0_1^+	1.441				8		57	39	22(2)
		0_2^+	0.389				510		6	4	13(5)
		2_1^+	0.901			104	16	135	12	100	100(5)
		2_2^+	0.510			0.3	77	0.06	3	2	<25
	3_1^+	2_1^+	0.901			6	43	8	31	167	96(6)
		2_2^+	0.404	-2	$M1,E2$	54	1330	6	17	100	100(2)
110	2_2^+	0_1^+	0.814				47		20	55	35(4)
		2_1^+	0.440	-8.6	$-4.6^{+1.9}_{-1.2}$	3	1830	0.5	37	100	100(3)
	2_3^+	0_1^+	1.214				8		27	100	100(7)
		0_2^+	0.267				1060		2	7	24(4)
		2_1^+	0.841			57	13	59	7	249	63(16)
		2_2^+	0.401			0.2	190	0.03	2	9	28(12)
		4_1^+	0.294				620		2	6	
	3_1^+	2_1^+	0.838			4	75	4	38	141	58(10)
		2_2^+	0.399			27	2200	3	27	100	100(10)
		4_1^+	0.292			22	660	1	2	9	10(1)
	4_2^+	2_2^+	0.585				1670		139	100	100(6)
		4_1^+	0.478			4	1050	0.7	32	23	62(9)

TABLE III. (*Continued*).

A	J_i^π	J_f^π	E_γ	δ		$B(M1)$	$B(E2)$	$W_\gamma(M1)$	$W_\gamma(E2)$	Relative intensities	
				Calc.	Expt.					Calc.	Expt.
112	2_2^+	0_1^+	0.737				90		24	94	44(4)
		2_1^+	0.388			31	2070	3.2	22	100	100(7)
	2_3^+	0_1^+	1.140				3		7	4	
		0_2^+	0.250				574		0.7	0.4	
		2_1^+	0.792			122	167	107	63	100	100
	3_1^+	2_1^+	0.748			11	120	8	34	168	91(7)
		2_2^+	0.360			43	2960	3.5	22	100	100(11)
		4_1^+	0.213			37	865	0.6	0.5	4.3	3.6(9)
114	2_2^+	0_1^+	0.694				71		14	78	66(3)
		2_1^+	0.362			21	1965	2	15	100	100(3)
	3_1^+	2_1^+	0.679			10	94	5.5	17	100	100(6)
		2_2^+	0.317			45	2580	2.5	10	57	84(3)
	4_2^+	2_2^+	0.626				1617		189	100	100(12)
		4_1^+	0.468			37	1068	7	29	19	33(8)
116	2_2^+	0_1^+	0.738				53		14	60	70(12)
		2_1^+	0.398			15	1810	2	22	100	100(16)
	3_1^+	2_1^+	0.726			8	71	5	18	100	100(41)
		2_2^+	0.329			44	2070	3	10	54	58(13)

From the decomposition of the wave functions in terms of F-spin and n_d-components (amplitude square), it turns out that these states have an FS character all along the isotopic chain and that, at least for the lighter isotopes, a close correspondence with states in column (a) of Fig. 1 exists. As an example, we show in Fig. 8 the structure of the even-spin yrast states up to $J=8$. For these states the amount of F-symmetry breaking is quite limited, except for the predicted 8^+ state in ^{102}Pd (this case will be discussed in the second part of this work).

In the lighter isotopes these states show a remarkable purity also with respect to the d-boson number; the n_d component which by far outweighs the remaing ones is that expected for a nucleus having a structure close to the U(5) limit. The purity decreases in the heavier isotopes, reflecting a slight change of their structure towards the O(6) limit where n_d is no longer a good quantum number.

We now discuss the e.m. properties of the states in order of increasing n_d.

(i) The calculations reproduce correctly the electric quadrupole moment of the 2_1^+ state, both in magnitude and sign, as well as the $B(E2)$ value of the $2_1^+ \rightarrow 0_1^+$ transition. The same comment applies to the magnetic dipole moment of the 2_1^+ state thereby justifying our choice of keeping the gyromagnetic factors g_π and g_ν to the same values found for the ruthenium chain.

(ii) All the states belonging to the $n_d=2$ triplet have been clearly identified in several isotopes. In ^{102}Pd, however, the possibility of interpretating the 2_2^+ state as a state of the triplet seems a little doubtful. Indeed, the calculations underestimate its energy (by 16% while reproducing that of the 4_1^+ state within 2%) as well as the values of the $B(M1;\ 2_2^+ \rightarrow 2_1^+)$ and $B(E2;\ 2_2^+ \rightarrow 0_1^+)$. The latter has an experimental value of the same order of magnitude as the $B(E2;\ 2_2^+ \rightarrow 2_1^+)$ whereas, at least in the U(5) limit, the $2_2^+ \rightarrow 0_1^+$ transition ($\Delta n_d = 2$) is forbidden.

The e.m. properties of the 4_1^+ state are well reproduced by the calculations. The values of the ratio $B(E2;\ 4_1^+ \rightarrow 2_1^+)/B(E2;\ 2_1^+ \rightarrow 0_1^+)$, measured in $^{102-110}$Pd, are scattered around an average value of about 1.6; they compare much better with the expectations of the U(5) limit (ranging from 1.6 to 1.78 for the different isotopes) than with those of the O(6) limit (ranging from 1.27 to 1.37).

The quadrupole moment of the 2_2^+ level, as well as $B(E2)$ values of the deexciting transitions show a fairly good agreement with the calculated data. It is interesting to observe that the experimental quadrupole moment, which has been measured in $^{106-110}$Pd, has the opposite sign of that of the 2_1^+ state, as expected in the U(5) limit. The calculated $B(M1;\ 2_2^+ \rightarrow 2_1^+)$ agree in order of magnitude with the experimental ones 10^{-3}–$10^{-4}\mu_N^2$ (see Table II). Since $M1$ transitions are forbidden between FS states, the $M1$ component in the $2_2^+ \rightarrow 2_1^+$ transition can only be explained on the basis of the MS components present in the wave functions of the 2_1^+ (see Fig. 8) and of the 2_2^+ state (for which the strength of the MS component varies from 0.02 to 0.10 in going from ^{104}Pd to ^{110} Pd). We notice that also the sign of the $E2/M1$ mixing ratio of the $2_2^+ \rightarrow 2_1^+$ transition is reproduced.

The good agreement between experimental and calculated values of the $B(E2)$ of the transitions deexciting the 0_2^+ level in $^{104-110}$Pd supports the interpretation of this state as lying within the IBA-2 model space and confirms our findings about the corresponding state in the ruthenium chain. The decomposition of the wave function of the 0_2^+ level in terms of F-spin components shows a quite pure FS character.
(iii) States belonging to the $n_d=3$ multiplet are clearly identified in most of the isotopes.

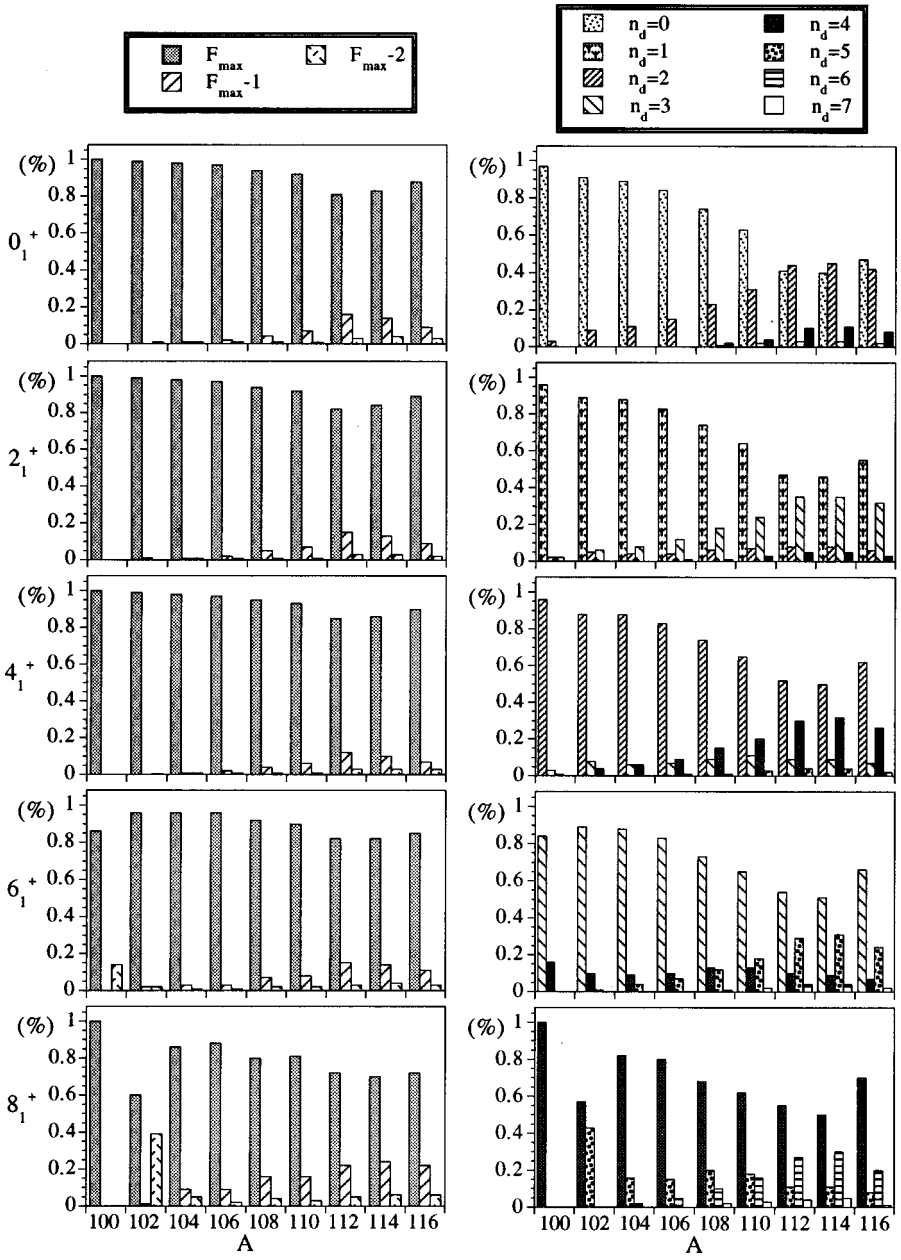

FIG. 8. *F*-spin components (left) and the four major n_d components (right) are reported for the $J=0$, 2, 4, 6, 8 yrast states as a function of the mass number for even palladium isotopes; the components of the $J=8$ state in ^{102}Pd are those of the 8_2^+ state (see second part of the present work for details). The *F*-spin and n_d components (amplitude square) are given as a percentage.

The e.m. properties of the 6_1^+ level are in general well reproduced. In particular, one might observe that in ^{110}Pd the calculated $B(E2)$ values for the transitions to the 4_1^+, 4_2^+, 4_3^+ levels are quite close to the experimental values which are scattered over three orders of magnitude (see Fig. 7).

In some isotopes up to three levels of spin 4 are known at an energy comparable to that of the 6_1^+ level, where only one state is expected in a model limited to FS states. On the basis of the decay properties it is possible to associate the 4_2^+ level with the FS state of the $n_d=3$ multiplet of Fig. 1. As to the comparison between experimental and calculated data of this state we only mention the close agreement for the quadrupole moment which has a particularly small absolute value.

The discussion about the levels of spin 3 and 2 belonging to the $n_d=3$ multiplet is postponed to the following section because it turns out that they are strongly mixed with states of the same spin and of lower symmetry.

The model completely fails to reproduce the preferential decay of the 0_3^+ level to the 2_1^+ level in $^{104-108}$Pd (see Fig. 9). Actually, for isotopes having a structure close to the U(5) limit, the $0_3^+ \rightarrow 2_1^+$ transition is forbidden. We are then led to conclude that this state lies outside the model space in spite of the reasonable agreement between experimental and calculated values of its excitation energy (see Fig. 5). The identification of a 0_4^+ state, very close in energy to the 6_1^+ state, in ^{104}Pd (at 2.103 MeV [26]) and in ^{106}Pd (at 2.001 MeV [27]) supports this conclusion. While in ^{104}Pd the decay of this state is not known, in ^{106}Pd its preferential decay to the 2_2^+ level closely matches the predictions of the 0_3^+ model state. In the heavier isotopes, starting from ^{110}Pd, the calcu-

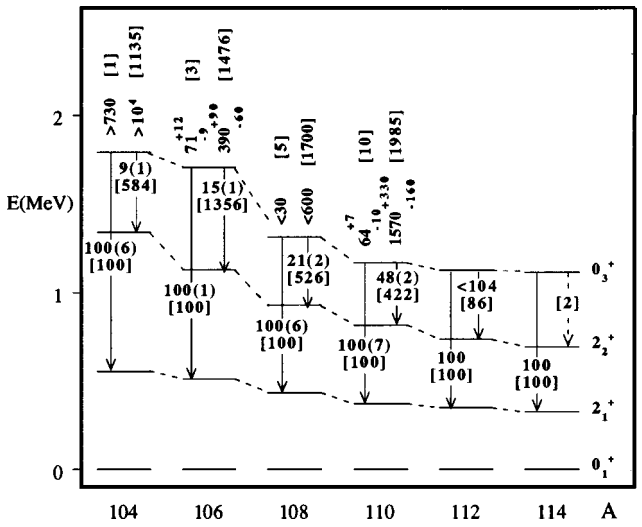

FIG. 9. Decay scheme of the 0_3^+ state in even palladium isotopes. Experimental and calculated (in square brackets) values for the intensity ratios are shown. Experimental and predicted $B(E2)$ values (in 10^{-4} e^2 b^2) are given in the upper part. No experimental value exists for the $0_3^+ \rightarrow 2_2^+$ transition in ^{114}Pd, indicated by a dashed line.

lations compare much better with the observed decay properties of the 0_3^+ states. In this case the preferential decay to the 2_1^+ state reflects the increasing importance of an O(6) structure characterized by selection rules which forbid the decay to the 2_2^+ level.

(iv) The experimental information on states belonging to the $n_d=4$ multiplet is rather limited so as to preclude the possibility of recognizing any systematic trend in their decay properties apart from the 8_1^+ state which is known in the whole chain.

The $B(E2)$ value of the $8_1^+ \rightarrow 6_1^+$ transition has been measured in $^{106-110}$Pd and is well reproduced by the calculations. The experimental value of the ratio $B(E2;\ 8_1^+ \rightarrow 6_1^+)/B(E2;\ 2_1^+ \rightarrow 0_1^+)$ suggests a structure of these isotopes still closer to the U(5) than to the O(6) limit. This is clearly seen in Fig. 10 where the experimental values of $B(E2)$ for the transitions of the yrast band, normalized to the $B(E2;\ 2_1^+ \rightarrow 0_1^+)$, are compared to the model predictions for FS states in the U(5) and O(6) limits [40].

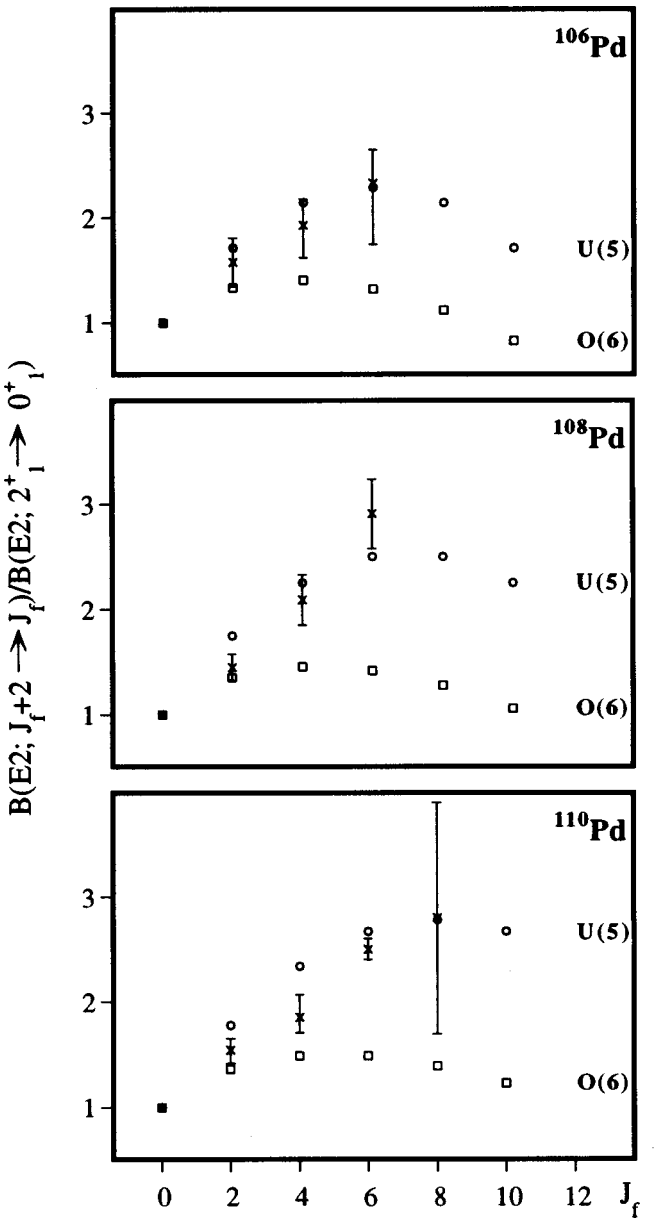

FIG. 10. Experimental values (crosses) of $B(E2)$ for the transitions in the yrast band, normalized to $B(E2;\ 2_1^+ \rightarrow 0_1^+)$, are given as a function of the spin of the final state. The model predictions in the U(5) (circles) and O(6) (squares) limits for the FS states are given for comparison.

B. $F=F_{\max}-1$ states

Having clarified which states have a predominant FS structure we can now proceed with some confidence to identify states having a predominant $F=F_{\max}-1$ character on the basis of their excitation energy and e.m. properties.

Referring again to Fig. 1, we will try to establish a correspondence with states of columns (a′) and (b′) since, as remarked in Sec. III, the calculated energies of the states reported in Fig. 5 do not depend on the Majorana parameter ξ_1.

First we consider the 2_3^+ and 3_1^+ states to check whether, like in ruthenium isotopes, they could be the lowest states having a large MS component. Due to the uncertainty in the identification of the candidates in ^{100,102}Pd we only consider the 2_3^+ and 3_1^+ states in $^{104-116}$Pd. Their energies are well reproduced by the calculations, where the choice of the Majorana parameters ξ_2 and ξ_3 plays a crucial role. As seen from Fig. 11, in the lighter isotopes the 2_3^+ and 3_1^+ states are predicted to have a quite pure $F_{\max}-1$ character and a main $n_d=1$ and $n_d=2$ component, respectively, so that the correspondence with the lowest state in columns (a′), (b′) of Fig. 1 is quite evident. In the heavier isotopes a large $F=F_{\max}$ component, which becomes predominant in ^{110}Pd, is present. The 2_3^+ state shares its MS character with the 2_4^+ state. Indeed, it turns out that the summed square amplitude of the $F_{\max}-1$ component for the 2_3^+, 2_4^+ states is close to one. This is also the case for the $F_{\max}$ component, meaning that no additional state with $J=2$ is significantly mixed with these states. Similar considerations apply for the 3_1^+, 3_2^+ states.

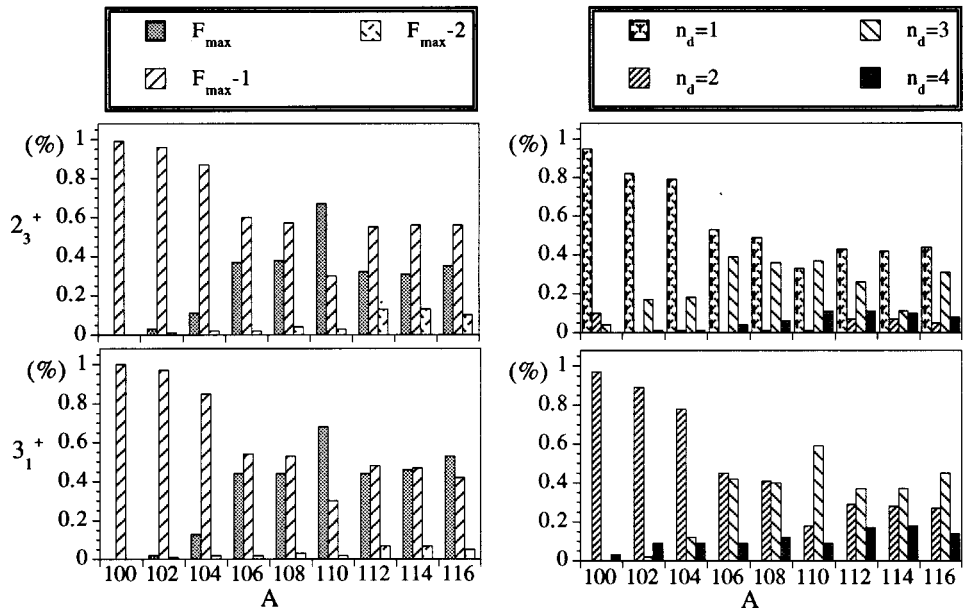

FIG. 11. F-spin components (left) and the four major n_d components (right) are reported for the 2_3^+, 3_1^+ states as a function of the mass number.

In $^{104-112}$Pd there is a large experimental information on the e.m. properties of the 2_3^+ state, which are all reasonably reproduced by the calculations. In particular we notice the importance of the large predicted $M1$ component in the $2_3^+ \rightarrow 2_1^+$ transition for reproducing the mixing ratio $\delta(2_3^+ \rightarrow 2_1^+)$, known in ^{106}Pd, as well as the intensity ratios in $^{104-112}$Pd (see Table III). Where the comparison is possible, namely in ^{104,106}Pd, the calculated values of $B(M1; 2_3^+ \rightarrow 2_1^+)$ are in agreement with the experimental data, whose order of magnitude is $10^{-2}\mu_N^2$.

This confirms our findings in the ruthenium chain, i.e., that in nuclei of the $A=100-120$ region the order of magnitude of $B(M1)$'s for transitions connecting a state of $F_{\max}-1$ character to a state of FS character with the same main n_d component is $10^{-2}\mu_N^2$. This value turns out to be one–two orders of magnitude larger than that found for the $2_2^+ \rightarrow 2_1^+$ transition.

The only information on the e.m. properties of the 2_4^+ level concerns its branching ratio in ^{106}Pd. A large percentage (0.35 in strength) of the $F_{\max}-1$ component is predicted in its wave function and also in this case the possibility of reproducing its preferential decay to the 2_1^+ level (see Table III) is due to the predominant $M1$ component in the $2_4^+ \rightarrow 2_1^+$ transition.

The information available on the 3_1^+ level concerns mixing ratios in $^{102-108}$Pd, intensity ratios in $^{104-110}$Pd and $B(E2)$'s in ^{110}Pd. As to ^{102}Pd, it seems difficult to draw any definite conclusion about the structure of the only known 3^+ level. Its energy (very close to that of the 6_1^+ state) compares well with that predicted for the 3_2^+ state (see Fig. 5) which has FS character; however, the only observed decay is to the 2_1^+ state in contradiction with this interpretation. On the other hand, the experimental limit for the mixing ratio of the transition ($\delta \geqslant 15$) compares better with the value predicted ($\delta=8$) for the $3_2^+ \rightarrow 2_1^+$ transition than with that predicted ($\delta=-0.9$) for the $3_1^+ \rightarrow 2_1^+$ transition. As to the other isotopes, a reasonable agreement is found between experimental and calculated data. We again stress the importance of the large $M1$ components predicted for the transitions to the 2_2^+ and 4_1^+ levels, which basically have two d-bosons, for reproducing the experimental data.

In several isotopes of the ruthenium chain it has been possible to find states which could be related to the $4^+,2^+,0^+$, $n_d=2$ triplet in column (a′) and to the $5^+,4^+,2^+$ $n_d=3$ triplet in column (b′) of Fig. 1. However, the lack of experimental data on their decay properties severely limited the comparison of experimental and calculated data.

The identification of the states belonging to the two triplets seems also possible in the palladium chain, where a larger body of spectroscopic data allows a more stringent comparison. On the basis of excitation energies (Fig. 5), possible candidates can be found in all isotopes, apart from ^{112}Pd.

First of all, we will discuss in detail the case of ^{106}Pd where it seems possible to associate the 4_4^+, 2_6^+, 0_5^+ and the 5_1^+, 4_3^+, 2_5^+ levels to the triplets $n_d=2$ of column (a′) and $n_d=3$ of column (b′) of Fig. 1, respectively. These states are displayed, together with those of lower energy, in Fig. 12 where thick lines indicate states of MS character and thin lines states of FS character. For the MS states are also reported the experimental and calculated intensity ratios of the deexciting transitions together with the available mixing ratios. It is particularly striking that the energy difference between the almost degenerate 4_4^+, 2_6^+, 0_5^+ triplet and the 2_3^+ level is very close to that between the 4_1^+, 2_2^+, 0_2^+ triplet and the 2_1^+ level.

The structure of the wave functions of the two triplets is given in Fig. 13. All states show a rather pure $F=F_{\max}-1$ character. The states having the same spin share partially their n_d components; the 5_1^+ level has a quite pure $n_d=3$ structure due to the fact that no additional 5^+ state is predicted at a nearby energy.

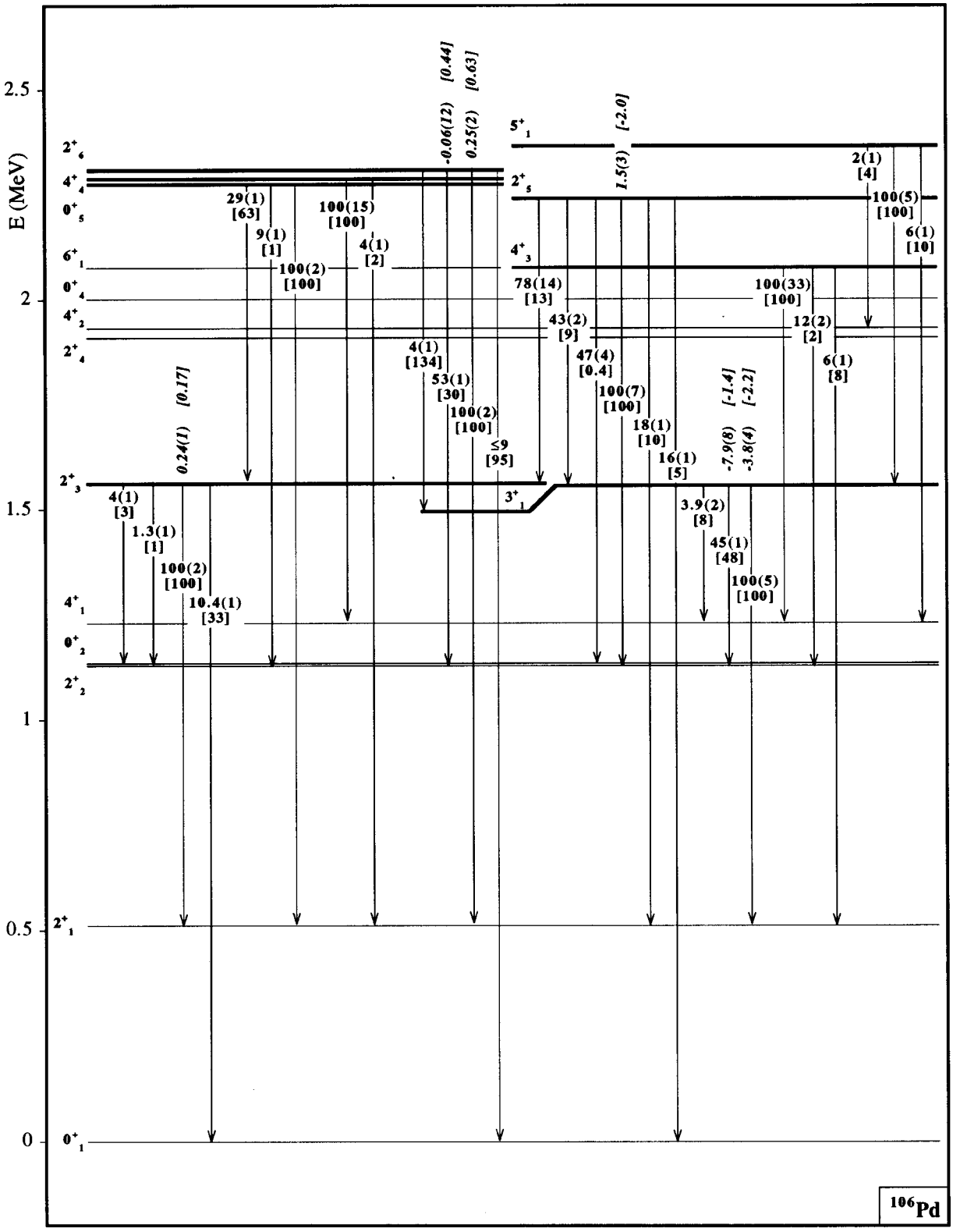

FIG. 12. Experimental intensity ratios for the states of ^{106}Pd marked by thick lines are compared to the calculated ones (in square brackets). Thick lines represent states of MS character, thin lines states of FS character. In italics are given the experimental values of the $E2/M1$ mixing ratios together with the calculated values in square brackets.

The decay properties of the two triplets are reasonably reproduced, including the small values of the mixing ratios of the transitions connecting these states to states of FS character. It is interesting to note that the magnitude of the predicted $B(E2)$ and $B(M1)$ reduced transition probabilities (see Table III) basically obey the selection rules mentioned above (Sec. II) which provide the signatures for the identification of MS states. Indeed, the order of magnitude of the $B(E2)$ values for the $0^+_5 \rightarrow 2^+_3$ and $5^+_1 \rightarrow 3^+_1$ transitions is that of an n_d-allowed transition connecting states having the

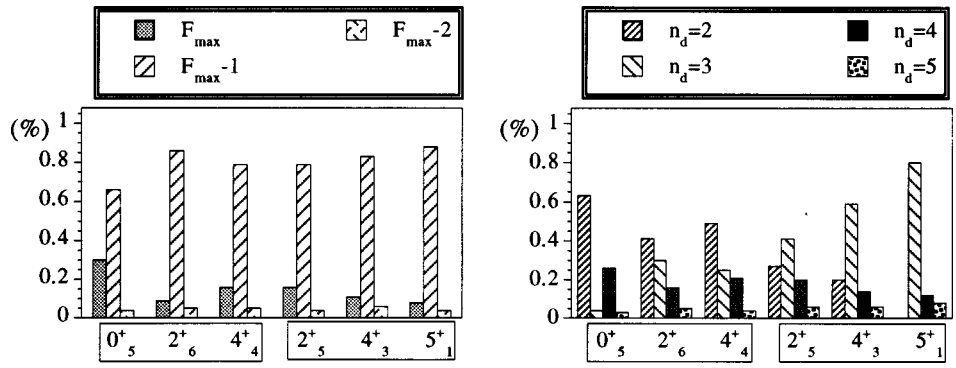

FIG. 13. F-spin components (left) and the four major n_d components (right) for the predicted 0_4^+, 2_5^+, 4_4^+ levels in ^{106}Pd which have been associated to the experimental 0_5^+, 2_6^+, 4_4^+ levels, respectively, and for the predicted 2_6^+, 4_3^+, 5_1^+ levels which have been associated to the experimental 2_5^+, 4_3^+, 5_1^+ levels. The triplets 0^+, 2^+, 4^+ and 2^+, 4^+, 5^+ are characterized by the main n_d component being equal to 2 and 3, respectively.

same F-spin [e.g., $B(E2;\ 2_1^+ \rightarrow 0_1^+)$] and is much larger than that of the $B(E2)$ values for the transitions connecting the 0_5^+ and 5_1^+ levels to states of FS character [e.g., $B(E2;\ 0_5^+ \rightarrow 2_2^+)$]. Moreover, the fact that the strongest transition deexciting the 4_3^+ and 4_4^+ levels is the one to the 4_1^+ level (which has basically an $n_d=2$ structure) appears to be due to the large $n_d=2$ component present in their wavefunctions (Fig. 13). Indeed, the predicted $B(M1)$ value for the $4_3^+ \rightarrow 4_1^+$, $4_4^+ \rightarrow 4_1^+$ transitions is comparable to that of the $2_3^+ \rightarrow 2_1^+$ transition.

In ^{104}Pd the states associated to the experimental 4_4^+, 0_5^+ and 4_3^+, 2_5^+ levels have a structure similar to that of the corresponding states in ^{106}Pd, shown in Fig. 13, with a higher degree of purity in terms of F-spin and n_d components. Thereby, the remarks made above for ^{106}Pd apply also to this isotope. The experimental e.m. data concerning the branching ratios of these states and the mixing ratios of the transitions from the 4_3^+, 4_4^+ states to the 4_1^+ state compare reasonably well with the calculated data (see Table III).

Also in ^{108}Pd and ^{110}Pd three 4^+ levels have been observed at an energy rather close to that of the 6_1^+ level. In ^{108}Pd they can be accounted for on the basis of the 4_2^+ level having a predominant FS character ($F_{\max}$ component = 0.90 in strength) and the 4_3^+, 4_4^+ levels a predominant $F_{\max}-1$ character ($F_{\max}-1$ component $\geqslant 0.71$ in strength). A similar interpretation is also possible for the corresponding states in ^{110}Pd even though the correspondence with the 4^+ states of the $n_d=3$ and $n_d=2$ MS triplets is not as straigthforward as in the lighter isotopes due to a large mixing in both the F-spin and n_d components. The comparison of experimental and calculated $B(E2)$'s of the transitions deexciting these levels in both isotopes is satisfactory. In ^{110}Pd, where the quadrupole moments of these states are known, calculations are able to reproduce the order of magnitude as well as the opposite sign of Q for the 4_3^+, 4_4^+ states.

Due to the lack of experimental data, it is not possible, in general, to recognize the presence of states which could be associated to U(5) states having $F=F_{\max}-1$ and $n_d>3$. However, in those few cases where it is, the model predictions account for an observed number of $J \geqslant 5$ states larger than that expected in a picture limited to FS states.

In particular, in ^{106}Pd, in addition to the 5_1^+ level discussed above, two more 5^+ states are known at an energy close to that of the 8_1^+ level; their excitation energies (Fig. 5) as well as their branching ratios, shown in the upper part of Fig. 14, are well reproduced. For nine of the ten transitions connecting the 5_2^+, 5_3^+ levels to lower lying states of spin $J=4,\ 5,\ 6$ the presence of an $M1$ component has been experimentally established (see column 6 of Table III). The calculations also predict a sizable $M1$ component though, in some cases, the sign of the mixing ratio is not reproduced. These states, as shown in the lower part of Fig. 14, can be interpreted basically as a mixture of the $n_d=4$, FS state and of the $n_d=4$, MS state of column (b′) in Fig. 1.

In ^{110}Pd the calculations correctly predict two $J=6$ states (6_2^+ and 6_3^+) at an energy close to that of the 8_1^+ level and two $J=8$ states (8_2^+ and 8_3^+) at an energy close to that of the 10_1^+ level (see Fig. 5). From the analysis of the structure of these states (Fig. 15) it seems possible to associate the experimental 6_2^+ and 6_3^+ levels to the $J=6$ states of the $n_d=4$, FS multiplet and of the $n_d=4$, MS multiplet of column (b′) in Fig. 1, respectively. This interpretation is supported by the capability of the calculations to reproduce (Fig. 7) the large $B(E2)$ values of transitions that, in our picture, are allowed, like the $6_2^+ \rightarrow 4_2^+$, $6_3^+ \rightarrow 4_3^+$ transitions ($\Delta F=0$, $\Delta n_d=1$), as well as the small $B(E2)$ values of transitions that are ''forbidden,'' like the $6_2^+ \rightarrow 4_1^+$ transition ($\Delta n_d=2$) or hindered because of the compensation effects mentioned in Sec. II, like the $6_3^+ \rightarrow 6_1^+$ transition ($\Delta F=1$). As to the structure of the 8^+ states, their $F_{\max}$ and $F_{\max}-1$ components have a comparable amplitude, the $n_d=5$ component being the largest one in both states. The two states can be interpreted basically as a mixture of the two $J=8$ states of the $n_d=5$, FS multiplet and of the $n_d=5$, MS multiplet in column (b′) of Fig. 1. The values of $B(E2;\ 8_2^+ \rightarrow 6_2^+)$, $B(E2;\ 8_3^+ \rightarrow 6_3^+)$, which are comparable to that of $B(E2;\ 2_1^+ \rightarrow 0_1^+)$, as well as those of $B(E2;\ 8_3^+ \rightarrow 6_2^+)$, $B(E2;\ 8_3^+ \rightarrow 8_2^+)$, which are smaller by one and two order of magnitude, respectively, are well reproduced by the calculations (Fig. 7). This implies that the model is able to evaluate correctly the amount of $F_{\max}$, $F_{\max}-1$ mixing in the 6_2^+, 6_3^+ and 8_2^+, 8_3^+ states.

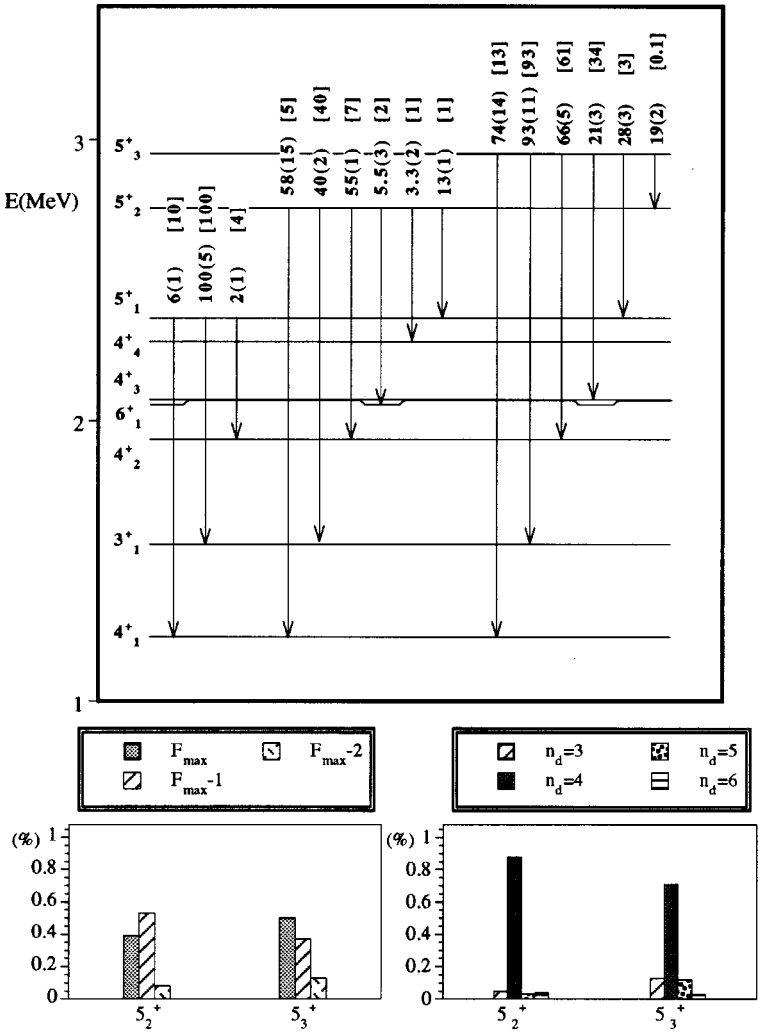

FIG. 14. Upper part: experimental and calculated values for the intensity ratios from the 5_1^+, 5_2^+ and 5_3^+ levels in ^{106}Pd. The main deexciting transitions from the 5_2^+ level to the 4^- state and from the 5_3^+ level to the 4_5^+ state, at 2.350 MeV (which lies outside the model space, see text), are not reported. Lower part: *F*-spin components (left) and four major n_d components (right) for the 5_2^+, 5_3^+ levels in ^{106}Pd.

Recently, Kim *et al.* [10], in a study of even palladium isotopes performed in the framework of the IBA-2 model, found that in some isotopes the 2_3^+ state has a predominant MS character as well as the 3_1^+ state in ^{104,106}Pd. The comparison of their results with those of the present work is difficult since they use a different type of Hamiltonian and keep the Majorana parameters at the values $\xi_1=0.2$, $\xi_2=0.4$–0.5 and $\xi_3=0$ MeV.

VI. CONCLUSIONS

In the present work we discuss the results of numerical calculations performed in the U(5) limit of the IBA-2 model which enabled us to identify groups of $F=F_{\max}-1$ states for which the eigenvalues of the generalized Majorana operator can be expressed in analytic form.

By using these results as a guideline, we have investigated

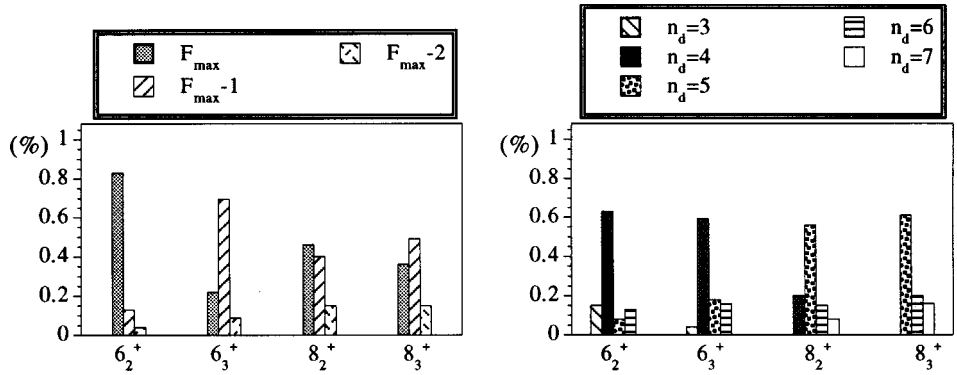

FIG. 15. *F*-spin components (left) and the four major n_d components (right) for the 6_2^+, 6_3^+ and the 8_2^+, 8_3^+ levels in ^{110}Pd.

the chain of even palladium isotopes ($^{100-116}$Pd) with the aim of identifying states of MS character. Starting from the Hamiltonian already used in the analysis of even ruthenium isotopes [7], we have optimized the values of the parameters by taking into account the excitation-energy patterns as well as the available experimental data on e.m. properties. In the analysis, six out of twelve parameters present in the Hamiltonian and in the $M1$ and $E2$ operators have been varied smoothly as a function of the mass number; they all turn out to be quite close to the values we adopted for the corresponding isotones in the ruthenium chain. Particular attention has been paid to the choice of the Majorana parameters ξ_2 and ξ_3 which play a decisive role in determining the excitation energy of MS states.

Excitation energies, magnetic dipole and electromagnetic quadrupole moments, $B(M1)$ and $B(E2)$ reduced transition probabilities, as well as $E2/M1$ mixing ratios and intensity ratios have been considered and compared to the calculated ones. A general good agreement has been found.

In most cases it has been possible to recognize a structure of the relevant states close to that of FS or MS states belonging to the U(5) limit of the model. This is particularly evident in the lighter isotopes of the chain.

All along the isotopic chain, predicted states of quite pure FS character and structure close to that of states belonging to the $n_d=2,\ 3,\ 4$ multiplets of the U(5) limit, have been successfully associated to experimental states. Only in the lighter isotopes the decay properties of the 0_3^+ state do not fit those predicted for the 0^+ state of the $n_d=3$ multiplet, so that it has to be considered an ''intruder'' state.

In most of the isotopes of the chain the 2_3^+, 3_1^+ levels have been identified as the lowest states having a large $F_{\max}-1$ component. In addition, in several isotopes, given experimental levels can be reasonably associated with states belonging to the two $n_d=2$, $J=4,\ 2,\ 0$ and $n_d=3$, $J=5,\ 4,\ 2$ triplets in the U(5) limit. In particular, for the first time, 0^+ states of $F_{\max}-1$ character have been identified in ^{104,106}Pd. In some cases it has also been possible to recognize the presence of $F=F_{\max}-1$ states having a predominant $n_d>3$ component, so that the model predictions can account, in the proper energy range, for an observed number of $J \geqslant 5$ states larger than that expected in a picture restricted to FS states.

Finally, from our overall analysis of ^{110,112,114}Cd [5,6], $^{98-114}$Ru [7], $^{100-116}$Pd (present work), it seems possible to conclude that the interpretation, in the framework of the IBA-2 model, of whole groups of states as having a predominant $F=F_{\max}-1$ is well-founded.

ACKNOWLEDGMENTS

Many thanks are due to I. Talmi for his interest in our work. We are grateful to A. Gelberg and R. Herzberg for providing us with the routine for the decomposition of the model wave functions in terms of *F*-spin components. Many thanks are also due to G. Maino for helpful discussions.

[1] A. Arima and F. Iachello, Phys. Rev. Lett. **35**, 1069 (1975).
[2] F. Iachello and A. Arima, *The Interacting Boson Model* (Cambridge University Press, Cambridge, England 1987) and references therein.
[3] A. Arima, T. Otsuka, F. Iachello, and I. Talmi, Phys. Lett. **66B**, 205 (1977).
[4] T. Otsuka, A. Arima, F. Iachello, and I. Talmi, Phys. Lett. **76B**, 139 (1978).
[5] A. Giannatiempo, G. Maino, A. Nannini, A. Perego, and P. Sona, Phys. Rev. C **44**, 1508 (1991).
[6] A. Giannatiempo, A. Nannini, A. Perego, and P. Sona, Phys. Rev. C **44**, 1844 (1991).
[7] A. Giannatiempo, A. Nannini, P. Sona, and D. Cutoiu, Phys. Rev. C **52**, 2969 (1995).
[8] A. Giannatiempo, A. Nannini, and P. Sona, in *Proceedings of the Ninth International Symposium on Capture Gamma-ray Spectroscopy and Related Topics*, Budapest, 1996, edited by G.L. Molnár, T. Belgya, and Zs. Révay (Springer-Verlag, Budapest, 1997), p. 35.
[9] P. Van Isacker and G. Puddu, Nucl. Phys. **A348**, 125 (1980).
[10] K. Kim, A. Gelberg, T. Mizusaki, T. Otsuka, and P. von Brentano, Nucl. Phys. **A604**, 163 (1996).
[11] J. Stachel, P. Van Isacker, and K. Heyde, Phys. Rev. C **25**, 650 (1982).
[12] P. Van Isacker, K. Heyde, J. Jolie, M. Waroquier, J. Moreau, and O. Scholten, Phys. Lett. **144B**, 1 (1984).
[13] I. Talmi, *Simple Models of Complex Nuclei* (Harwood Academic, Switzerland, 1993).
[14] T. Otsuka, N. Yoshida, Program NPBOS Japan Atomic Energy Research Institute report JAERI-M85-094 (1985).
[15] I. Talmi, Phys. Lett. B **405**, 1 (1997).
[16] C. De Coster and K. Heyde, Int. J. Mod. Phys. A **4**, 3665 (1989).
[17] P.O. Lipas, P. von Brentano, and A. Gelber, Rep. Prog. Phys. **53**, 1353 (1990).
[18] P. Van Isacker, K. Heyde, J. Jolie, and A. Sevrin, Ann. Phys. (N.Y.) **171**, 253 (1986).
[19] O. Scholten, K. Heyde, P. Van Isacker, J. Jolie, J. Moreau, M. Waroquier, and J. Sau, Nucl. Phys. **A438**, 41 (1985).
[20] A. Giannatiempo, G. Maino, A. Nannini, and P. Sona, Phys. Rev. C **48**, 2657 (1993).
[21] O. Scholten, Ph.D. thesis, University of Groningen, 1980.
[22] K.S. Krane and R.M. Steffen, Phys. Rev. C **2**, 724 (1970).
[23] B. Singh, Nucl. Data Sheets **81**, 1 (1997).
[24] D. De Frenne and E. Jacobs, Nucl. Data Sheets **63**, 373 (1991).
[25] J. Blanchot, Nucl. Data Sheets **64**, 1 (1991).
[26] M. Pignanelli *et al.*, Nucl. Phys. **A540**, 27 (1992).
[27] D. De Frenne and E. Jacobs, Nucl. Data Sheets **72**, 1 (1994).
[28] L.E. Svensson, C. Fahlander, L. Hasslgren, A. Bäcklin, L. Westerbeerg, D. Cline, T. Czosnyka, C.Y. Wu, R.M. Diamond, and H. Kluge, Nucl. Phys. **A584**, 547 (1995) and references therein.
[29] J. Blanchot, Nucl. Data Sheets **62**, 803 (1991).
[30] K. Pohl, P.H. Regan, J.E. Bush, P.E. Raines, D.P. Balamuth, D. Ward, A. Galindo-Uribarri, V.P. Janzen, S.M. Mullins, and S. Pilotte, Phys. Rev. C **53**, 2682 (1996).

[31] D. De Frenne and E. Jacobs, Nucl. Data Sheets **67**, 809 (1992).
[32] R. Hertberger *et al.*, Nucl. Phys. **A562**, 157 (1993).
[33] J.L. Durell, in *Proceedings of the International Conference on the Spectroscopy of Heavy Nuclei*, Crete, 1989, edited by J.F.Sharpey-Schafer and L. Skouras, IOP Conf. Ser. No. 105 (IOP, London, 1990).
[34] D. De Frenne, E. Jacobs, and M. Verboven, Nucl. Data Sheets **57**, 443 (1989).
[35] R. Aryaeinejad *et al.*, Phys. Rev. C **48**, 566 (1993).
[36] J. Blanchot and G. Marguier, Nucl. Data Sheets **75**, 739 (1995).
[37] J. Blanchot and G. Marguier, Nucl. Data Sheets **73**, 81 (1994).
[38] J.A. Grau *et al.*, Phys. Rev. C **14**, 2297 (1976).
[39] M. Luontama, R. Julin, J. Kantele, A. Passoja, W. Trzaska, A. Bäcklin, N.G. Jonsson, and L. Westerberg, Z. Phys. A **324**, 317 (1986).
[40] R.F. Casten and D.D. Warnes, Rev. Mod. Phys. **60**, 389 (1988).